

Development of Low Charge-to-Mass Ratio Post-Accelerator for the RIA Project[†]

P.N. Ostroumov

Physics Division, Argonne National Laboratory, 9700 S. Cass Avenue, Argonne, IL 60439, USA

Abstract. A post-accelerator for rare isotopes (RIB linac) which must produce high-quality beams of radioactive ions over the full mass range, including uranium, at energies above the coulomb barrier is being developed for the U.S. RIA facility. To provide highest possible intensity of rare isotopes with masses from 6 to 240, the linac will accept all ions in the 1+ charge state. A high resolution separator for purifying beams at the isobaric level precedes the RIB linac. Charge stripping in the linac takes place at two stages: helium gas stripping at energies of a few tens of keV/u, and an additional foil stripping at ~680-1700 keV/u for the heavier ions. The RIB linac will utilize existing superconducting heavy-ion linac technology for all but one exceptional piece, a very-low-charge-state injector, which is needed for the first ~9 MV of the accelerator. This section consists of a pre-buncher followed by three sections of cw, normally-conducting RFQ. The first section is a conventional RFQ operating at 12 MHz. The following two sections are hybrid RFQs operating at 12 and 24 MHz. A 1:2 scale cold model of 12 MHz RFQ was built and it is being studied in order to determine final specifications for the full power 12 MHz hybrid RFQ. This paper reports on the present status of the RIB linac development with particular attention paid to the very-low-charge-state injector section.

INTRODUCTION

An initial concept of the RIA post accelerator suitable for ions up to mass 132 has been described in ref. [1]. This paper presents a modified design of the RIB linac which must produce high-quality beams of radioactive ions over the full mass range, including uranium, at energies above the Coulomb barrier, and have high transmission and efficiency. The latter requires the RIB linac to accept at injection ions in the 1+ charge state [2]. A high resolution separator for purifying beams at the isobaric level precedes the RIB linac. The mass filtering process will provide high purity beams while preserving transmission.

The technology developed for existing superconducting heavy-ion linacs, characterized by excellent performance and a very high degree of modularity, provides a basis for all but a small portion of such an accelerator system. The exceptional piece is a very low charge state injector section. The most efficient generation of rare isotopes beams requires singly-charged ions at initial injection. Very-low-

charge-state ions can most efficiently be bunched and accelerated by using several sections of cw, normally-conducting RFQ for the first few MV of the RIB accelerator.

For best efficiency over the full mass range, helium gas stripping must be performed at different energies for different mass ions. The linac following this stripping can accelerate ions of charge to mass ratio 1/66 and above. For example, by stripping at 7 keV/u, some 55% of an incident ¹³²Sn beam can be stripped into a charge state 2+ and further accelerated [3]. For the heavier ions of Z>54, higher charge states are required, for which the best stripping efficiency is achieved at the higher energy of 20 keV/u.

The block-diagram of the RIB linac is shown in Fig. 1. It consists of the following main sections [2]:

- A high-resolution isobar separator.
- An injector with three sections of normally-conducting RFQs.
- A superconducting linac which will accelerate ions of $q/m > 1/66$ to 680 keV/u or more.
- A carbon-foil stripper at beam kinetic energy per nucleon $W_n > 680$ keV/u, when necessary, to provide a $q/m > 2/15$ for the last stage of acceleration. The beam energy at this point depends on the particular

[†] Work supported by the U. S. Department of Energy under contract W-31-109-ENG-38.

charge-to-mass ratio.

- A superconducting linac to accelerate ions of $q/m > 2/15$ to energies of 6 MeV/u or higher.

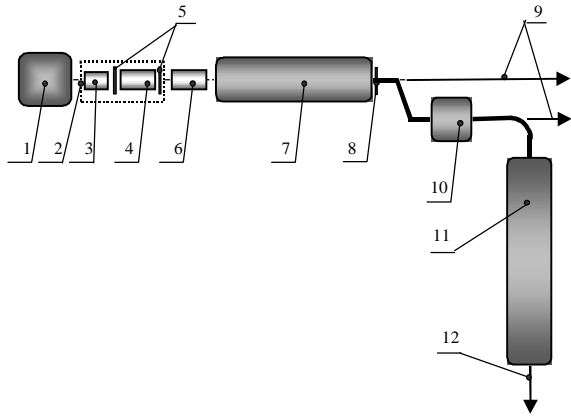


FIGURE 1. Block-diagram of the RIB Linac. 1 – Isobar separator, 2 – High voltage platform, 3 – 12 MHz RFQ, 4 – 12 MHz Hybrid RFQ, 5 – helium strippers, 6 – 24 MHz Hybrid RFQ, 7 – SC Linac between the strippers, 8 – carbon stripper, 9 – beams to astrophysics experiments, 10 – SC booster linac, 11 – ATLAS, 12 – high energy beams.

ISOBAR SEPARATOR

The first section consists of a high-resolving power mass separator system where the beam enters and exits at 100 keV in DC mode. We assume that at the entrance the beam has a transverse emittance of $10 \pi \text{ mm} \times \text{mrad}$ in both the vertical and horizontal planes; however, the beam width must be 1 mm in the horizontal and 8 mm in the vertical plane. This ensures a large span along the horizontal plane when the beam is inside the dipoles and an almost-parallel focusing along the vertical plane throughout the linac.

A diagram illustrating the layout and resolution of the spectrometer is shown in Fig. 2. There are two magnetic-bending sections that consist of mirror-symmetric dipoles. Each section is at a different potential. The first bend is at ground potential and is called Section H (between points A and C), since the beam is at the higher energy (100 keV). The mass of interest bends 60° at each dipole at 2.5 m radius. A multipole magnet set between the two dipoles corrects for the geometric aberrations up to 5-th order. A Monte Carlo simulation of the expected mass spectrum at point C is shown in the inset plot (a) where the mass difference ratio is $\Delta m/m = 1/20000$, and we assume that there is no energy spread in the beam and the phase space distributions are Gaussian. For a $\pm 10 \text{ eV}$ Gaussian spread in energy the resolution deteriorates as is shown in plot (b). To eliminate this effect

another bend has been applied by two immersion lenses at Section I (between points C and D), after the beam has decelerated from 100 to 10 keV. The lower energy bend at Section L (between points D and F) is almost identical to Section H; however, it is scaled down by a factor of $\sqrt{10}$ and floats at 90 kV to cancel the energy dispersion imposed by Section H. The spectrum shown in plot (c) is obtained at the section between points F and G where the beam has accelerated back up to 100 keV. The spectrum shows that there is a 5% contamination at the central peak from the adjacent ones. The method of calculation and details of the optics have been detailed by Portillo and others elsewhere [4].

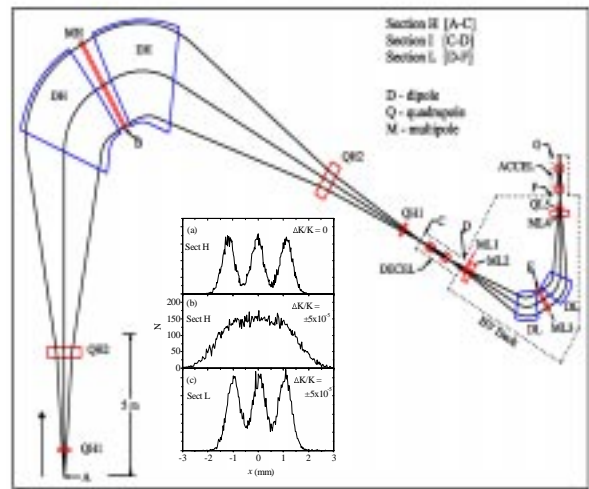


FIGURE 2. Layout of dual-potential spectrometer. The spectrometer can be broken up into 4 sections as described in the text. The inset shows a plot of the beam distribution at points C and F.

INJECTOR SECTION

The buncher, conventional 12-MHz RFQ and hybrid-RFQ sections, and both He-gas-stripper cells will be placed on a 380 kV open-air variable-voltage platform. Placing these elements on a variable-voltage platform allows operation with a fixed constant-velocity profile for the full mass range of ions, including uranium.

The 12-MHz gridded-gap, four-harmonic bunching system which is presently in use on the ATLAS accelerator may be most suitable for this application: this system can bunch approximately 75% of a dc beam into 1 nsec bunches, while maintaining excellent longitudinal emittance. However, the highest beam transmission can be obtained by using multi-harmonic

drift tube buncher (MHB).

The RFQ should operate at as low a frequency as is practicable to maximize the transverse focusing strength. As it has been demonstrated at ANL the split-coaxial RFQ geometry is appropriate for operation at 12 MHz [5]. The RFQ is designed for a minimum charge to mass ratio of 1/240: ions of higher charge state are accommodated by simply scaling both the platform voltage and the RFQ rf voltage to match. Table 1 presents the detailed parameters of the proposed low-frequency low-charge-state RFQ section. The cw vane voltage of 92 kV with a mean bore radius of 9 mm has been proven entirely practical in extensive tests of the prototype 12-MHz RFQ at ANL. Numerical simulations of the beam dynamics through the MHB and RFQ sections have been performed. Two electrostatic quadrupole triplets are used for beam matching between the buncher and RFQ. The proposed design achieves longitudinal emittance as low as $0.2 \pi \text{ keV/u} \times \text{nsec}$ for 80% of cw beam entering the buncher.

TABLE 1. RFQ Basic Parameters.

Parameter	Value
Operating frequency	12.125 MHz
Charge-to-mass ratio	1/6-1/240
Input energy	2 keV/u
Output energy	7.12 keV/u
Inter-Vane voltage	92 kV
R_0	9 mm
Synchronous phase	-25°
Peak surface electric field	128 kV/cm
Number of cells	57
Length	2.2 m
Transverse normalized acceptance	$0.4 \pi \text{ mm} \times \text{mrad}$

Hybrid RFQ

High-efficient acceleration of well bunched ion beams will be performed in the proposed hybrid RFQ (H-RFQ) structure [6]. We found that the concept of separated accelerating and focusing zones can be applied to the acceleration of heavy ions with $q/m \geq 1/240$ and at very low energies if the beam focusing is provided by rf quadrupoles. The DTL accelerating and rf focusing sections can be integrated into a single resonant structure we call the hybrid RFQ. The proposed hybrid RFQ structure has the following innovative features compared to conventional RFQs with similar parameters [6]: a) separate sections of drift tube accelerator and rf focusing structures placed inside the same resonant structure producing twice the accelerating gradient; b) focusing provided by four rf quadrupoles operating as a triplet; c) lower rf power consumption per unit

length; d) lower peak surface electric fields and less surface area at high electric field.

Rf quadrupoles will be used for heavy ion beam focusing in ‘triplet’ mode. An unmodulated four-vane RFQ forms two sections each with length $\beta\lambda$ separated by a drift space $\beta\lambda/2$. The focusing strength of each RFQ lens with length $\beta\lambda/2$ is adjusted and fixed by the aperture radius R_0 . A section of the RFQ with length $\beta\lambda$ acts as a “doublet”. The drift space between the “doublet” is necessary to ease the required electric field between the vanes. The whole focusing system works as a symmetric triplet.

Basic design parameters of the H-RFQ are given in Table 2. The beam dynamics design of the H-RFQ structure was performed in two steps: 1) preliminary design of the longitudinal layout and 2) detailed simulation of beam dynamics in 3D electric fields. These steps were iteratively repeated in order to achieve design goals: minimal emittance growth, lowest possible peak surface field, lowest sensitivity to the misalignments and rf field errors, and maximum possible 6D acceptance. The first DT section of the H-RFQ operates at zero synchronous phase while the last two DT sections operate at -20° synchronous phase. The 1+ rare isotope beams come from either standard ISOL-type ion sources or a helium gas catcher and, therefore, the maximum expected transverse normalized emittance is quite low, $\sim 0.1 \pi \text{ mm} \times \text{mrad}$. Heavy beams such as uranium will be formed with even lower normalized emittances, $\sim 0.01 \pi \text{ mm} \times \text{mrad}$.

The simulations show that the beam parameters such as average energy, phase spread, emittances, Twiss parameters, etc. experience negligible change if the voltage is varied in the range -3% to +7% of the nominal value.

TABLE 2. Design Parameters of the H-RFQ-1.

Parameter	Value
Operating frequency	12.125 MHz
Charge-to-mass ratio	1/6-1/240
Input energy	7.12 keV/u
Output energy	20.3 keV/u
Inter-Vane voltage	100 kV
RFQ aperture radius	1.14-1.23 mm
Number of drift tubes in three sections	13-10-13
Peak surface electric field	118 kV/cm
Length	3.34 m
Transverse normalized acceptance	$0.3 \pi \times \text{mm} \times \text{mrad}$
Resonator quality factor	10800
Calculated rf power consumption	11.6 kW

Several resonant structures have been considered as candidates for the H-RFQ. The main specifications for our application are: 1) the structure length $\sim 3.34 \text{ m}$ is

determined by the given input and output beam energies; 2) the structure should be mechanically stable; and 3) the shunt impedance should be high. Though split-coaxial structures have been used in several low frequency RFQs, the Wideroe-type structure better satisfies the abovementioned conditions. The plan view of the accelerating structure is shown in Fig. 3. According to the 3D electromagnetic simulation code CST MWS, the rf losses in this copper cavity are 11.6 kW at 100 kV inter-vane voltage. The losses are lower than in split-coaxial RFQ of similar length because the total capacitive loading of the drift tubes is about half that of the four-vane structure.

To determine complete engineering specifications, an aluminum 1:2 model of the H-RFQ for the RIA RIB linac was built (see Fig. 4). A uniform voltage distribution on all vanes and drift tubes was measured, as shown in Fig. 5.

Another H-RFQ operating at 24.25 MHz will be designed for acceleration of ions with lowest charge-to-mass ratio 1/66 in the energy range from 20 keV/u to 62 keV/u. Numerical simulations of the beam dynamics through the entire chain of RFQ sections have been performed. A preliminary study using linear codes shows that beam matching between the RFQ sections, including stripping, is straightforward, and can be achieved without any emittance growth in either the transverse or the longitudinal phase plane. Several rf bunchers are required for the matching purpose. Transverse focusing in the transitions can be done with either electrostatic quadrupoles or SC solenoids.

SUPERCONDUCTING LINAC

The low-charge-state injector linac can be based on established interdigital drift-tube SC niobium cavity designs, which can provide typically 1 MV of accelerating potential per cavity in this velocity range [1]. The low-charge-state beams, however, require stronger transverse focusing than used in existing SC ion linacs. For the charge states considered here ($q/m = 1/66$) the proper focusing can be reached with the help of strong SC solenoid lenses with fields up to 15 T. Commercial vendors now offer a wide range of high field magnets in the range of 10 to 17 Tesla.

The SRF linac consists of 54 interdigital four-gap cavities operating at -20° synchronous phase, and each cavity is followed by a SC solenoid. This linac can accelerate any beam with $q/m \geq 1/66$ over the velocity range $0.0011 \leq \beta \leq 0.04$.

After the second stripper, the desired charge state must be selected and further accelerated to the beam

velocity required to match to the ATLAS linac section in order to provide the last stage of acceleration to the desired beam energy. The solid line in Fig. 6 shows the average charge state as a function of the atomic number of the ion beam. The calculations were made taking into account the beam kinetic energy at the location of the second stripper.

The post-stripper section of the RIB linac will be designed for the acceleration of multiple-charge-state beams to enhance the available beam intensities for experiments. As it was shown in [7] a wide range of the charge spread $\Delta q/q$, about 20%, can be accepted and accelerated in the ATLAS accelerator. We have restricted the possible range of $\Delta q/q$ to $\leq 11\%$ in order to avoid emittance halo in the phase space. The dots in Fig. 6 presents a possible range of charge states Δq

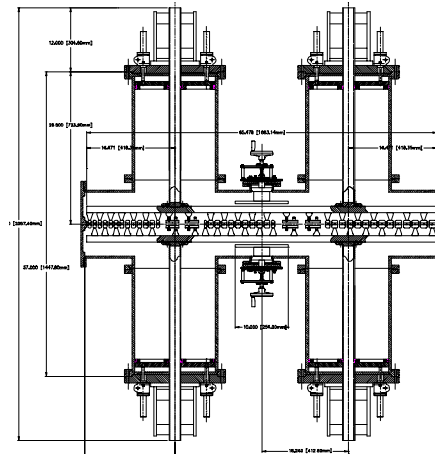


FIGURE 3. Plan view of the 1:2 cold model of the 12 MHz hybrid RFQ.



FIGURE 4. Photograph of the 1:2 cold model of the 12 MHz hybrid RFQ.

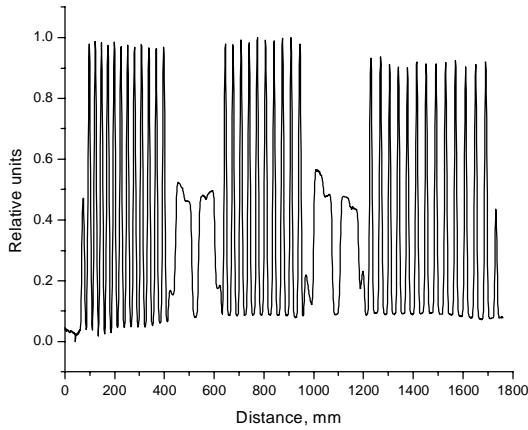


FIGURE 5. Electric field distribution along the H-RFQ cold model obtained by bead-pull measurements.

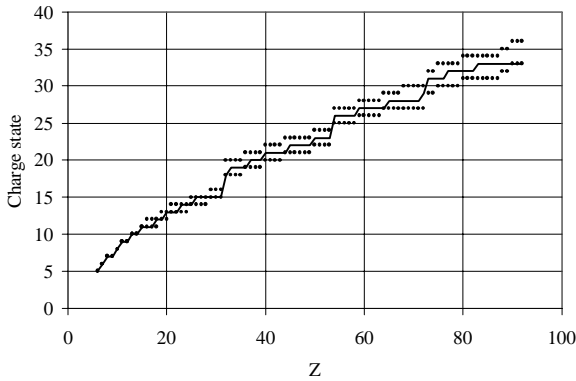


FIGURE 6. Charge states of heavy ions as a function of atomic number after the passage through the carbon stripper. The solid curve shows the most probable charge state. The dots show the range of charge states accepted for further acceleration.

acceptable for the following acceleration. As a consequence of multiple-charge-state acceleration the total stripping efficiency is significantly higher than for the single charge-state beams, as can be seen in Fig. 7. The RIB linac of the RIA Facility will produce beam intensities higher by a factor of ~ 25 as compared with post-accelerators based on an ECR charge breeder. However, the transverse and longitudinal emittances of multi- q beams will be larger by a factor of ~ 3 as it follows from beam measurements in ATLAS [7].

Further acceleration by eight SRF cavities of $\beta_G = 0.037$ is required in order to bring the beam energy to approximately 1.4 MeV/u and match the velocity acceptance of the $\beta_G = 0.06$ resonators in ATLAS. The present ATLAS configuration is being enhanced by

adding new SC cavities.

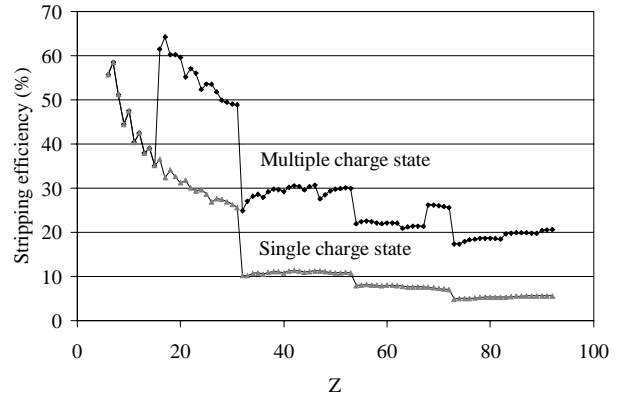


FIGURE 7. RIB linac overall stripping efficiency in the regime of single and multiple charge state beam acceleration.

REFERENCES

1. Shepard, K.W., and Kim, J.W., "A Low-Charge-State Injector Linac for ATLAS" in *Proceedings of the 1995 IEEE Particle Accelerator Conference*, Dallas, TX, IEEE, 0-7803-3053, Vol. 2, pp. 1128-1130, 1996.
2. Ostroumov, P.N., Nolen, J.A., Pardo, R.C., Shepard, K.W., Kolomiets, A.A., "Design of a Post Accelerator for the Rare Isotope Accelerator Facility" in *Proceedings of the 2001 IEEE Particle Accelerator Conference*, edited by P. Lucas and S. Webber, Chicago, IL, June 18-22, 2001, pp. 4080-4082.
3. Decrock, P., Kanter, E.P., and Nolen, J.A., *Rev. Sci. Instrum* **68**, 2322 (1997).
4. Portillo, M., Nolen, J.A., and Barlow, T.A., "Design Layout of an Isobar Separator Based on 5th Order Calculations" in *Proceedings of the 2001 IEEE Particle Accelerator Conference*, edited by P. Lucas and S. Webber, Chicago, IL, June 18-22, 2001, pp. 3015-3017.
5. Shepard, K.W., Kaye, R.A., Clift, B.E., and Kedzie, M., "Beam Tests of the 12 MHz RFQ RIB Injector for ATLAS" in *Proceedings of the 1999 IEEE Particle Accelerator Conference*, edited by A. Luccio and W. MacKay, March 29-April 2, 1999, NYC, pp. 525-527.
6. Ostroumov, P.N., and Kolomiets, A.A., "New Concept for Acceleration of Slow, Low-Charge-State Heavy Ion Beams" in *Proceedings of the 2001 IEEE Particle Accelerator Conference*, edited by P. Lucas and S. Webber, Chicago, IL, June 18-22, 2001, pp. 4077-4079.
7. Ostroumov, P.N., Pardo, R.C., Zinkann, G.P., Shepard, K.W., Nolen, J.A., *Physical Review Letters* **86**, N 13, March 2001, pp. 2798-2801.